INSTITUTE OF PLASMA PHYSICS

NAGOYA UNIVERSITY

RESEARCH REPORT

NAGOYA, JAPAN

THRESHOLD OF ELECTROMAGNETIC INSTABILITY IN A MAGNETIC NEUTRAL SHEET

Kaoru Yamanaka

IPPJ-301 August 1977

Further communication about this report is to be sent to the Research Information Center, Institute of Plasma Physics, Nagoya University, Nagoya, Japan

---

Present Address: JAERI, Tokai-Mura, Ibaraki, JAPAN

Abstract

The structure of electromagnetic perturbations in a magnetic neutral sheet is analyzed within the framework of Vlasov-Maxwellian picture. In reference to Harris' equilibrium state, a boundary value problem is formulated and solved to give the possible existence of a low-frequency electromagnetic wave of compressional mode, propagating along the electron-drift current in the sheet. The stability of this mode is critically dependent on the thickness parameter of the sheet. If the sheet is thin enough, the perturbation will grow even for $T_e=T_i$. The critical thicknesses are calculated with regard to various temperature ratios and their values are found to be about 0.9 r^*_{Li} or less, where r^*_{Li} means the ion Larmor radius just outside the sheet region.

1. Introduction

The magnetic field configurations with neutral sheet structure (or the state where another component of the field exists) can be found in a wide range of plasma physics; for example, sun spot magnetic field [1, 6-10], geomagnetic tail [2, 11-14], neutral sheets or points of laboratory plasma [3, 4] and tokamaks [5]. At such configurations effective conversion of magnetic energy to thermal energy of plasmas occurs. The change of the topology of magnetic fields, the so-called reconnection process, plays a main role in this efficient energy conversion.

The phenomena of neutral-point discharge [6] have long attracted the astrophysicists. The first MHD model of this dynamical dissipation process was proposed by Sweet [1] and critically examined by Parker [7] for the explanation of the large amount of the released energy and rapid reconnection rate. The model was further developed by Petschek [8] and Friedman and Hamberger [9]. The basic idea of these models is that the reconnection is caused by the plasma flow towards the magnetic null plane from both sides of the neutral layer. The neutral point is thought to become highly turbulent or dissipative due to microinstabilities [9]. Then the magnetic field lines are reconnected at the neutral point. This idea was numerically examined by Yeh and Axford [10]. The amount of the dissipated energy and the reconnection time scale are considered to be controlled by the outer conditions of the layer because the energy source is the plasma flow towards the null

point from the outer region.

There exists another problem that is the thinning of the neutral sheet before the onset of the reconnection process. This phenomenon was observed in the geomagnetic tail [2] and in a laboratory [3]. In the geomagnetic tail the plasma sheet at about 15 R_E (earth radius) far from the earth is reduced in its thickness to about 1 R_E. In the laboratory experiment the thickness of the current sheet becomes as thin as about the ion Larmor radius just before the occurrence of the abrupt destruction of the sheet. Relating this phenomenon the instability in the neutral sheet must be investigated. Tearing mode has a difficulty to explain the abrupt destruction of the sheet because the sheet can be stable in much longer time than that expected by the tearing mode theory [3]. Furthermore the nonlinear theories [11, 12] show the tearing mode can be stabilized at very small level of the turbulence. Schindler [13] proposed the theory of the ion tearing instability, which was recently developed and applied to the magnetic substorm by Galeev and Zelenyi [12, 14]. For the occurrence of the ion tearing instability, the normal component of the magnetic field to the null plane is necessary. Its strength to trigger the instability is restricted within a certain range and in the other range the ion tearing mode does not exist even when the sheet thickness is thin enough.

In this paper we show that the thin sheet becomes unstable against a mode which is different from the tearing mode. Considered is the magnetically compressional mode that is propagating perpendicularly to the magnetic field lines. The

instability of this mode is examined with regard to the sheet thickness within the framewark of Vlasov-Maxwellian picture. Detailed behavior of particles near the null plane is considered and those ions with meandering orbits are shown to play an important role in triggering the instability. The obtained dispersion relation is estimated numerically and analytically. We show the mode becomes unstable when the thickness of the sheet is reduced to about the order of the ion Larmor radius.

2. Equilibrium configuration and particle orbits

Consider a magnetic neutral sheet of plane configuration, and take a coordinate system whose x-axis coinsides with the normal to the sheet. (Fig.1) A background magnetic field $\underset{\sim}{B}_0$ is assumed to be parallel and antiparallel to the z-axis for $x>0$ and $x<0$, respectively. On the yz-plane at $x=0$, which is referred to as the null plane, the magnetic field vanishes. The configuration can be described by a vector potential $\underset{\sim}{A}_0=(0, A_0(x), 0)$, with a magnitude function $A_0(x)$ having its mimimum at $x=0$, since

$$\underset{\sim}{B}_0 = \nabla \times \underset{\sim}{A}_0 = (0, 0, dA_0(x)/dx) \quad . \tag{1}$$

The motion of a plasma particle in this equilibrium configuration is characterized by three constants of motion, i.e., the y- and z-components of canonical momentum and the kinetic energy, because the magnetic field is only dependent on x and no external electric field is considered. If v_x, v_y and v_z are the velocity components of a particle of species j (ion

or electron) with mass m_j and charge e_j, then it is convenient to define the following quantities, both having the dimension of velocity,

$$\varepsilon = (v_x^2 + v_y^2)^{1/2} \quad , \tag{2}$$

$$p = s_j v_y + eA_0(x)/m_j c \quad . \tag{3}$$

Here $s_j = \mathrm{sgn}(e_j)$, $e=|e_j|$ and c is the velocity of light. (The ions are assumed to be singly charged.) The quantity ε denotes the velocity perpendicular to the magnetic field, and p is proportional to the canonical momentum in the y-direction.

An equilibrium distribution function in the neutral sheet configuration was given by Harris [15] in a drift Maxwellian type,

$$F_j = n_0(2\pi v_j^2)^{-3/2} \exp\{-(\varepsilon^2 - 2s_j U_j p + v_z^2 + U_j^2)/2v_j^2\} \quad , \tag{4}$$

where n_0 is the number density of the plasma particles at the null plane. The thermal and drift velocity of j-species are denoted by v_j and U_j, respectively. The charge neutrality condition implies

$$U_e/T_e = -U_i/T_i \quad , \tag{5}$$

where $T_j = m_j v_j^2/2$ (j=i,e) is the temperature of j-species.

The distribution function F_j is substituted into Maxwell's equations and gives the equilibrium vector potential

$$\underset{\sim}{A}_0(x) = \underset{\sim}{e}_y \, 2 \frac{cT_i}{e|U_i|} \log \cosh \frac{x}{\lambda} \quad , \tag{6}$$

where the half-thickness of the sheet $\lambda = \sqrt{2}(c/|U_i|)\lambda_D$ is

defined in relation to the Debye length $\lambda_D=[T_i/\{(1+T_e/T_i)\times \times(4\pi n_0 e^2)\}]^{1/2}$. From this potential the magnetic field is derived,

$$\underset{\sim}{B}_0(x) = \underset{\sim}{e}_z\{8\pi n_0(T_i+T_e)\}^{1/2}\tanh(x/\lambda) \quad . \tag{7}$$

The particle density is distributed in space as

$$n(x) = n_0 \mathrm{sech}^2(x/\lambda) \quad . \tag{8}$$

These equilibrium solutions are shown in Fig.1. The thickness of the plasma sheet is now related to the drift velocity by

$$r^*_{Li}/\lambda = \frac{1}{2}|U_i|/v_i \quad , \tag{9}$$

where r^*_{Li} is the ion Larmor radius far outside the sheet region

$$r^*_{Li} = v_i m_i c/eB_0(x\to\infty) \quad .$$

The ratio (9) plays a crucial role in our argument concerning the threshold of the electromagnetic instability at the sheet.

It can be shown that the particle orbits in such a neutral sheet is classified into two groups [16]. Since v_x^2 is positive, the allowed region is defined in (ε, p) space from (2) and (3)

$$\varepsilon > | p - A_j(x) | \quad , \tag{10}$$

where $A_j(x) = \frac{e}{m_j c} A_0(x)$ (Fig.2). This implies that for given ε and p, the particle motion is bounded in a finite range of x-space. In the case of

$$0 < p - \varepsilon \quad ,$$

each particle has two turning points, x_1 and x_2, in the same (positive or negative) x-half plane (region II in Fig.2). This kind of orbits are called "non-crossing orbits", since these particles never cross the x=0 plane. If on the contrary,

$$p - \varepsilon < 0$$

holds, the two turning points are situated symmetrically on both sides of the null plane (region I in Fig.2). They are given x_1 and $-x_1$. This kind of particles can go back and forth across the magnetic null plane. The orbits of this type are called "meandering orbits". These two groups are shown in Fig.3. The meandering orbits are proper to the magnetic neutral sheet and have some remarkable characteristics. Firstly, the drift velocity can change its sign according to values of ε and p. Secondly, when the electric field is present along the y-axis, the meandering particles are accelerated and run in the y-derection in a similar way to the case of no external magnetic field. The hybrid behavior of the meandering particles, i.e. partly like gyrating particles and partly like free particles, is essential when we consider the perturbation in the neutral sheet.

3. Derivation of the wave equation

When we consider the perturbation at the null plane, it is necessary to deal with the kinetic equation because of the effect of the finite Larmor radius. To avoid the complicated characteristics of the kinetic equation, we convert the usual velocity space to (ε, p) space. Three components of the

velocity $\underset{\sim}{v}$ are written in terms of the constants of the motion (2), (3);

$$v_x = \pm[\varepsilon^2 - \{p - A_j(x)\}^2]^{1/2} \equiv \sigma W \quad ,$$

$$v_y = s_j\{ p - A_j(x)\} \quad , \tag{11}$$

$$v_z = v_z \quad ,$$

where $\sigma = \mathrm{sgn}(v_x)$.

Assuming that the collisional effect is negligible in the neutral sheet, we get a linearized Vlasov equation in terms of the zeroth order constants ε and p :

$$\partial f^j/\partial t + \underset{\sim}{v}[\varepsilon, p, A_j]\cdot\nabla_r f^j + (e_j/m_j)\{\delta\underset{\sim}{E} + c^{-1}\underset{\sim}{v}[\varepsilon, p, A_j]\times\delta\underset{\sim}{B}\}\cdot\nabla_v F_j = 0 \quad , \tag{12}$$

where f^j is the linearized deviation of the distribution function and $\delta\underset{\sim}{E}$, $\delta\underset{\sim}{B}$ are the perturbed electric and magnetic fields, respectively. The three components of the operator ∇_v denote that

$$\frac{\partial}{\partial v_x} = \sigma W \frac{1}{\varepsilon}\frac{\partial}{\partial \varepsilon} \quad ,$$

$$\frac{\partial}{\partial v_y} = s_j \frac{\partial}{\partial p} + s_j\{p - A_j(x)\}\frac{1}{\varepsilon}\frac{\partial}{\partial \varepsilon} \quad , \tag{13}$$

$$\frac{\partial}{\partial v_z} = \frac{\partial}{\partial v_z} \quad ,$$

and $\underset{\sim}{v}[\varepsilon, p, A_j(x)]$ is given by eq.(11). Though the external magnetic field does not appear explicitly in eq.(12), its effect is included in the quantity $\underset{\sim}{v}[\varepsilon, p, A_j(x)]$ through the term $A_j(x) = (e/m_j c)A_0(x)$.

In the present equilibrium given by eq.(4), all of the zeroth order quantities are varying along x-coordinate but they are uniform in y- and z-directions. Consequently we can make Fourier-expansion of eq.(12) with respect to variables y and z, and carry out the Laplace transformation with respect to time t. Then we have a linear differential equation

$$\partial f^j_{k\omega}/\partial x - i\sigma W^{-1}\{\omega - k_z v_z - k_y v_y[p,\ A_j]\}\ f^j_{k\omega}$$
$$= \sigma W^{-1}[-(e_j/m_j)\{\delta \underset{\sim}{E}_{k\omega} + c^{-1}\underset{\sim}{v}[\varepsilon,\ p,\ A_j]\times\delta \underset{\sim}{B}_{k\omega}\}\cdot\nabla_v F_j + f^j_k(t=0)], \tag{14}$$

where suffices k, ω denote the Fourier-Laplace transformed quantities and $f^j_k(t=0)$ is the initial perturbation of the distribution function. This equation has a solution

$$f^j_{k\omega}(x;\sigma) = \sigma\int_{x_1}^{x} d\xi W^{-1}[-(e_j/m_j)\{\delta \underset{\sim}{E}_{k\omega} + c^{-1}\underset{\sim}{v}[\varepsilon,\ p,\ A_j]\times\delta \underset{\sim}{B}_{k\omega}\}\cdot\nabla_v F_j$$
$$+ f^j_k(t=0)]\exp[i\sigma\Phi(x,\ \xi)] + C_\sigma \exp[i\sigma\Phi(x,\ x_1)], \tag{15}$$

where

$$\Phi(x,\xi) \equiv \int_{\xi}^{x} \frac{\omega - k_z v_z - k_y s_j\{p - A_j(x')\}}{W[\varepsilon,\ p,\ A_j(x')]}\, dx' \quad . \tag{16}$$

C_σ is an integration constant to be determined and x_1 is an arbitrary position of reference. The quantity $\Phi(x,\xi)$ describes the Doppler shifted phase variation along the unperturbed orbit. When x is equal to x_1 in eq.(15), we have

$$f^j_{k\omega}(x_1;\ \sigma) = C_\sigma \ .$$

In general $f^j_{k\omega}$ takes a different value for a different σ and so

does C_σ. But when the constant x_1 represents one of the turning points, where W = 0 holds, $f^j_{k\omega}(x_1;\ \sigma=1)$ and $f^j_{k\omega}(x_1;\ \sigma=-1)$ should have the same value, because v_x vanishes. Then we can replace C_σ by C in eq.(15) if x_1 is chosen as a turning point. The same argument can be applied to the other turning point x_2, and the relation $f^j_{k\omega}(x_2;\ \sigma=1)=f^j_{k\omega}(x_2;\ \sigma=-1)$ determines the constant C.

On the other hand the perturbed electric and magnetic fields $\delta\underset{\sim}{E}$ and $\delta\underset{\sim}{B}$ can be represented by a vector and a scalar potentical, $\delta\underset{\sim}{A}$ and $\delta\phi$, as

$$\delta\underset{\sim}{E} = -\nabla\delta\phi - c^{-1}\partial\delta\underset{\sim}{A}/\partial t \quad , \tag{17}$$

$$\delta\underset{\sim}{B} = \nabla \times \delta\underset{\sim}{A} \quad .$$

When we choose the Lorentz gauge

$$\nabla\cdot\delta\underset{\sim}{A} + c^{-1}\partial\delta\phi/\partial t = 0 \quad , \tag{18}$$

the wave equation is given by

$$\nabla^2\delta\underset{\sim}{A} - c^{-2}\partial^2\delta\underset{\sim}{A}/\partial t^2 = -(4\pi/c)\underset{\sim}{j} \quad . \tag{19}$$

The exchange of energy between waves and plasma occurs only when the y-component of the perturbed electric field is finite, because in the present configuration the current due to electrons is the only candidate for the energy source. One of the examples of such energy-exchange mechanisms is the collisionless tearing mode [17]. The wave-vector of this mode is along the magnetic field lines, and the electric field is uniformly excited along the y-axis. Accordingly, this mode is purely growing and has no threshold of the instability. Since

we are looking for the triggering action caused by the thinning of the sheet, we analyze another perturbation. Considered here is the mode whose wave-vector is directed along the electric current.

Suppose the perturbed vector potential is given by

$$\delta\underset{\sim}{A} = \underset{\sim}{e}_y \, \delta A(x) \, \exp[i(ky-\omega t)] \quad , \tag{20}$$

where we write k instead of k_y. The other components of the vector potential are reasonably assumed to be negligibly small. Using the relation (17) and the Lorentz gauge (18), we write the electric and the magnetic fields

$$\delta\underset{\sim}{E} = \begin{bmatrix} -(ck/\omega)\, d\delta A(x)/dx \\ i(\omega/c - ck^2/\omega)\, \delta A(x) \\ 0 \end{bmatrix} , \qquad \delta\underset{\sim}{B} = \begin{bmatrix} 0 \\ 0 \\ d\delta A(x)/dx \end{bmatrix} . \tag{21}$$

This is the magnetically compressional mode with a non-vanishing electric field component in y-direction. In other words, this mode is a coupled one of a transverse wave (δE_x, δB_z) and a longitudinal wave δE_y. Considering (21) and using the relation $f^j_{k\omega}(x_2;\ \sigma=1) = f^j_{k\omega}(x_2;\ \sigma=-1)$, we can determine the value of the constant C;

$$C = -(e_j/m_j)[\sin\Phi(x_2,x_1)]^{-1} \int_{x_1}^{x_2} d\xi W^{-1} g^j_{k\omega}[\varepsilon,\ p,\ A_j(\xi)] \cos\Phi(x_2,\xi)$$

$$+ (e_j/m_j)\{s_j c^{-1} \partial F_j/\partial p + (ck/\omega)\varepsilon^{-1} \partial F_j/\partial\varepsilon\}\delta A(x_1) \quad , \tag{22}$$

where

$$g^j_{k\omega} = [(ck^2/\omega) - kc^{-1} s_j\{p - A_j(\xi)\}][s_j \partial F_j/\partial p + (\omega/k)\varepsilon^{-1} \partial F_j/\partial\varepsilon]$$

$$\times\ \delta A(\xi) + f^j_k(t=0) \quad . \tag{23}$$

Eq.(15) with eq.(22) gives the perturbed distribution function

$$f^j_{k\omega}(x;\sigma)=(e_j/m_j)\{s_j c^{-1}\partial F_j/\partial p+(ck/\omega)\varepsilon^{-1}\partial F_j/\partial\varepsilon\}\delta A(x)$$
$$+i\sigma(e_j/m_j)\int_{x_1}^{x} d\xi W^{-1} g^j_{k\omega}\exp[i\sigma\Phi(x,\xi)]$$
$$-(e_j/m_j)[\sin\Phi(x_2, x_1)]^{-1}\exp[i\sigma\Phi(x, x_1)]$$
$$\times\int_{x_1}^{x_2} d\xi W^{-1} g^j_{k\omega}\cos\Phi(x_2,\xi) \quad . \tag{24}$$

The first term of eq.(24) is derived from the transverse components of the perturbation, δE_x and δB_z. The other terms represent the coupled effect of the longitudinal component δE_y and the transverse components. This effect is caused by the inhomogeneity due to the sheet structure.

The wave equation (19) is finally expressed by introducing the perturbed distribution function

$$d^2\delta A(x)/dx^2+\{\omega^2/c^2-k^2+2\lambda^{-2}\mathrm{sech}^2(x/\lambda)\}\delta A(x)$$
$$=\sum_j 2s_j\omega_{pj}^2/(cn_0)\int d\varepsilon\, dp\, dv_z\, W^{-1}\varepsilon(p-A_j)$$
$$\times[\int_{x_1}^{x} d\xi W^{-1} g^j_{k\omega}\sin\Phi(x,\xi)\delta A(\xi)$$
$$+\cos\Phi(x,x_1)[\sin\Phi(x_2,x_1)]^{-1}\int_{x_1}^{x_2} d\xi W^{-1} g^j_{k\omega}\cos\Phi(x_2,\xi)\delta A(\xi)]. \tag{25}$$

This is the integro-differential equation which must be solved as an eigenvalue problem. The operator in the left hand side (LHS) is the same as the one appearing in the equation of collisionless tearing mode if one puts $\omega=0$ and replaces k by k_z, because the LHS comes only from the transverse component of

the perturbation quite similarly in situation to the tearing mode. The RHS represents the perturbed current which is derived from the coupled effect of the electromagnetic and the electrostatic components. This perturbed current has a maximum value at the magnetic null plane and decreases with the distance from the plane. There are poles coming from the second term in the square bracket, that is

$$\Phi(x_2, x_1) = n\pi \qquad (n=0, \pm1, \pm2, \cdots) \quad . \tag{26}$$

In the case of homogeneous magnetic field, the integrated phase $\Phi(x_2, x_1)$ can easily be obtained and the condition (26) reduces simply to that of cyclotron resonances.

4. Approximate estimate of the orbit-integral

Now we consider the case where the phase integral is sufficiently small, $\Phi(x_2, x_1) \ll 1$. This is satisfied by the approximation of low frequency. This condition will be given later explicitly. As to this perturbation the first term in the RHS of eq.(25) is much smaller than the second term.

The perturbed amplitude of the vector potential $\delta A(x)$ has its maximum value at the null plane, because a strong energy exchange between particles and waves takes place near the plane. In Fig.4 contour lines of the distribution function F_i are depicted. This shows that the source term of eq.(25) is mostly contributed by the particles situated very close to the null plane, even in the case where the ratio λ/r^*_{Li} is as small as or less than unity. Therefore, we may expand the amplitude

$\delta A(\xi)$ in the integrand of eq.(25) around $\xi=0$,

$$\delta A(\xi) = \delta A(0) + \frac{1}{2}\xi^2 \delta A''(0) + \cdots \quad . \tag{27}$$

This corresponds to take a symmetrical mode with respect to x=0 plane. It can be shown that the anti-symmetrical mode does not exist under the condition of small phase integral. Taking the first term of this expansion, we can get a second order differential equation from the wave equation (25). In general the orbit-integral cannot be carried out analytically. An approximation for the background magnetic field, however, enables us to integrate this term.

In the vicinity of the magnetic null plane, $|x|/\lambda \ll 1$, the equilibrium magnetic field (7) varies linearly along the x-axis as

$$B_0(x) = B_{max}\, x/\lambda \quad , \tag{28-a}$$

and far from the plane, $|x|/\lambda \gg 1$, the field strength becomes almost constant

$$B_0 = B_{max} \quad . \tag{28-b}$$

Therefore our equilibrium may be devided into two regions; the inner region and the outer region (Fig.5). In the inner region, $|x| \leq \lambda$, the field varies linearly and passes through zero at x=0, while in the outer region, $\lambda \leq |x|$, the field has the constant value. The phase integral $\Phi(x_2, x_1)$ now can be calculated in both regions. In the outer region, the particle orbits are circles and have no drift velocity, then we have

$$\Phi(x_2, x_1) = \pi\omega/\omega^*_{cj} \quad , \tag{29}$$

where $\omega^*_{cj} = eB_{max}/m_j c$. In the inner region there are two kinds of orbits and the integral must be estimated separately in each group. For the meandering orbits

$$\Phi(x_1, -x_1) = -\left(\frac{2}{h_j \varepsilon}\right)^{1/2} \{ (\omega - s_j k\varepsilon) K(\kappa_1) + 2 s_j k\varepsilon E(\kappa_1) \} . \quad (30\text{-a})$$

For the noncrossing orbits

$$\Phi(x_2, x_1) = -\{h_j(\varepsilon+p)\}^{-1/2} \{ (\omega - s_j kp) K(\kappa_2) + s_j k(\varepsilon+p) E(\kappa_2) \} . \quad (30\text{-b})$$

where $\kappa_1^2 = (\varepsilon+p)/2\varepsilon$, $\kappa_2 = \kappa_1^{-1}$, $h_j = v_j^2/(|u_j|\lambda^2)$ and K, E are the complete elliptic integrals of the first and the second kind, respectively. When we compare eq.(30) with eq.(29), we see that in the inner region the role of gyrofrequency ω^*_{cj} in the homogeneous magnetic field is played by the quantity $(\omega^*_{cj}\omega_b)^{1/2}$, where ω_b denotes the bounce frequency v_i/λ around the magnetic null plane. Then the condition of the small phase-integral can be given here explicitly;

$$\omega \; / \; (\omega^*_{ci}\omega_b)^{1/2} \ll 1 \quad .$$

The orbit-integral with respect to ξ is the RHS of eq.(25) is now carried out analytically. The final form of the wave equation in this approximation is

$$d^2\delta A(x)/dx^2 + \lambda^{-2}\{2\,\mathrm{sech}^2(x/\lambda) - m^2\}\delta A(x) = J(x;\omega,k)\delta A(0) \quad , \quad (31)$$

where $m^2 = \lambda^2(k^2 - \omega^2/c^2)$. The source term $J(x; \omega, k)$ is given, in the inner region,

$$J(x;\ \omega,\ k)= \sum_j (2/cn_0)k_{Dj}^{\ 2}(U_j-\omega/k)$$

$$\times\int_0^\infty d\varepsilon\int_{p_\ell}^{p_u} dp\int_{-\infty}^{\infty} dv_z s_j\varepsilon(p-h_jx^2)\{\varepsilon^2-(p-h_jx^2)^2\}^{-1/2}[ck^2\omega^{-1}$$

$$-kw_D(\varepsilon,\ p)c^{-1}][\omega-kw_D(\varepsilon,\ p)]^{-1}F_j(\varepsilon,\ p,\ v_z)\quad , \qquad (32\text{-a})$$

where $A_j(x)$ is written by h_jx , $k_{Dj}^{\ 2}=4\pi n_0e^2/T_j$, $p_\ell=-\varepsilon+h_jx^2$ and $p_u=\varepsilon+h_jx^2$. In the outer region, on the other hand, the source term is vanishing,

$$J(x;\ \omega,\ k) = 0\quad . \qquad (32\text{-b})$$

Now, in the inner region the particles drift perpendicularly to the magnetic lines of force. The averaged drift velocity during one bounce period is denoted by $w_D(\varepsilon,\ p)$ in eq.(32-a). Explicit forms of $w_D(\varepsilon,\ p)$ are given as follows; for the meandering particles

$$w_D^m = s_j\varepsilon[1-2E(\kappa_1)/K(\kappa_1)]\quad , \qquad (33\text{-a})$$

and for the noncrossing particles

$$w_D^n = s_j\varepsilon[2\kappa_2^{-1}\{1-E(\kappa_2)/K(\kappa_2)\} - 1]\quad . \qquad (33\text{-b})$$

5. Solutions of the wave equation and the dispersion relation

In the outer region, where (32-b) holds, the wave equation (31) is satisfied by the associated Legendre function of degree 1 and order m[18]. As for the boundary condition when x tends to infinity, we put

$$A^{out}(x\to\infty) = 0.$$

Then we get a solution applicable to the outer region

$$\delta A^{out}(x) = c_1 P_1^{-m}[\mu(x)] \quad , \tag{34}$$

where $\mu(x) \equiv \tanh(x/\lambda)$ and m denotes only positive quantity. The solution of the collisionless tearing mode has a similar form to the present solution. On the other hand, the solution in the inner region, where the source term $J(x; \omega, k)$ is present, is given by

$$\delta A^{in}(x) = \{c_2 P_1^m[\mu(x)] + c_3 Q_1^m[\mu(x)]\}\delta A(0) + \delta A(0)\int_0^x G(x;\eta)J(x;\omega,k)d\eta \quad . \tag{35}$$

The propagator appearing in the integrand is

$$G(x;\eta) = \lambda\{\Gamma(2-m)/\Gamma(2+m)\}\{Q_1^m[\mu(x)]P_1^m[\mu(\eta)] - P_1^m[\mu(x)]Q_1^m[\mu(\eta)]\} \quad , \tag{36}$$

where $\Gamma(z)$ is the Gamma function. The constants c_2 and c_3 are determined by the boundary conditions at x=0;

$$\delta A^{in}(0) = \delta A(0) \quad ,$$
$$d\delta A^{in}(0)/dx = 0 \quad .$$

Then the constants are given by

$$c_2 = -2^{-m}\pi^{1/2}\{\Gamma(\tfrac{3}{2} - \tfrac{1}{2}m)/\Gamma(1+\tfrac{1}{2}m)\}\sin(\tfrac{1}{2}m\pi) \quad ,$$

$$c_3 = -2^{1-m}\pi^{-1/2}\{\Gamma(\tfrac{3}{2} - \tfrac{1}{2}m)/\Gamma(1+\tfrac{1}{2}m)\}\cos(\tfrac{1}{2}m\pi) \quad .$$

These solutions should be connected smoothly at the boundary of two regions, i.e.

$$\delta A^{out}(\lambda) = \delta A^{in}(\lambda) \quad ,$$

and

$$d\delta A^{out}(\lambda)/dx = d\delta A^{in}(\lambda)/dx \quad .$$

should be satisfied. From these conditions we can get a dispersion relation,

$$\{P_1^{-m}[\mu(\lambda)]\}'\{P_1^{-m}[\mu(\lambda)]\}^{-1}$$
$$=[c_2\{P_1^m[\mu(\lambda)]\}'+c_3\{Q_1^m[\mu(\lambda)]\}'+\int_0^\lambda \{G(x;\eta)\}'J(\eta;\omega,k)d\eta]$$
$$\times [c_2\{P_1^m[\mu(\lambda)]\}+c_3\{Q_1^m[\mu(\lambda)]\}+\int_0^\lambda G(x;\eta)J(\eta;\omega,k)d\eta]^{-1} \quad , \tag{37}$$

where prime denotes the first derivative with respect to x. This is an exact but implicit form of the dispersion relation for the magnetically compressional mode in the field structure of Fig.5. To pick up the dominant terms in the RHS of eq.(37), we drop the terms smaller than the order m($m<<1$). Then the relation becomes

$$\{Q_1^m(0)\}^{-1}[Q_1^m[\mu(\lambda)]/\mu(\lambda)-\mu(\lambda)/(1-\{\mu(\lambda)\}^2)]$$
$$=\int_0^\lambda J(\eta;\omega,k)[1+\{\mu(\lambda)-1/\mu(\lambda)\}\{\mu(\eta)-\mu(\lambda)\}]d\eta \quad . \tag{38}$$

The LHS of this equation represents the dispersive characteristics of the mode. To evaluate the real part of the RHS, we take the first dominant term and assume that the phase velocity is slower than the ion drift velocity; $\omega_r/k<<|U_i|$. It should be noted, however that in our reference system ions are not at rest but are drifting at the speed U_i. When we integrate eq.(38) the contribution from such part of the meandering particles that travel beyond the boundary, $x=\pm\lambda$, may be included,

since this will give little effect on the result. The contribution of the noncrossing particles to the current integral is found to be smaller than that of the meandering particles. This implies that a gyrating (noncrossing) particle cannot move so easily as a meandering particle does under the influence of the perturbed electric field. So, we can neglect the contribution of the noncrossing particles for the estimate of the real part. Consequently the real part of the dispersion relation, to determine ω_r, is given by

$$[Q_1^m[\mu(\lambda)]/\mu(\lambda)-\mu(\lambda)/(1-\{\mu(\lambda)\}^2)]/Q_1^m(0)$$

$$\simeq \sum_j \{\sqrt{2}\lambda^2/(\pi c)\}k_{Dj}^2(|U_j|/v_j)^{1/2}(U_j-\omega_r/k)\exp(-U_j^2/2v_j^2)$$

$$\times \{(ck/\omega_r)\alpha_j+c\beta_j/v_j\} \quad , \tag{39}$$

where

$$\alpha_j = (9\pi^2/16)2^{1/4}\Gamma(5/4)\,{}_1F_1(5/4,1;U_j^2/2v_j^2) \quad ,$$

$$\beta_j = -s_j(41\pi^2/48)2^{-1/2}\Gamma(3/4)\,{}_1F_1(3/4,1;U_j^2/2v_j^2) \quad ,$$

and ${}_1F_1(a,b;z)$ is the confluent hypergeometric function. Here we have assumed that $\omega_r/k \ll c$, $|U_i|/c \ll 1$ and $v_j/c \ll 1$. It should be noted that the eigenmode obtained here are concerned with both electrons and ions. This exhibits a remarkable contrast to the collisionless tearing mode which is related only with electrons.

The imaginary part of the current term comes from the pole, $\omega_r/k=w_D^{m,n}$. Both ions and electrons of the meandering orbits can couple with the perturbed field and exchange their

energies. As to the noncrossing particles, however, both species do not couple but only one, because each of them is drifting in a definite direction: when the phase velocity is positive the noncrossing ions couple but when the phase velocity is negative only electrons do. The ratio of the contribution from the noncrossing particles to that from the meandering particles is at most $(m_e/m_i)^{1/4}$, so that a major role in the energy exchange between the plasma and the waves is played by the meandering ions and electrons. The particles, which are traveling through the boundary $x=\pm\lambda$, will make a small but finite contribution to the imaginary part of the dispersion relation. If this contribution is not negligible, its effect on the growth rate calculation must be taken into account. But the relative influence of this effect is numerically estimated to be a few per cent, so that we can neglect it for the present consideration. With the assumption

$$|\gamma| << |\omega_r| \ ,$$

we can obtain the growth rate of the magnetically compressional mode along the current sheet,

$$\gamma \simeq \pi|\omega_r|\,[\textstyle\sum_j \zeta_j (U_j-\omega_r/k) I_j]/V \ , \qquad (41)$$

where

$$I_j = v_j^{-5/2} \int_{|\omega_r/k|}^{\infty} d\varepsilon \{R(\tilde{\kappa}_1)+H(s_j\omega_r/k)\tilde{\kappa}_2 R(\tilde{\kappa}_2)\} \ ,$$

$$R(\kappa)=\varepsilon^{1/2} K(\kappa) \tilde{J}(\varepsilon, s_j\omega_r/k) \exp[-\{\varepsilon^2-2s_jU_j(2\kappa^2-1)\varepsilon\}/2v_j^2] \ ,$$

$$\tilde{J}(\varepsilon,x)=8\kappa_3^2(1-\kappa_3^2)\ /\{4(1-\kappa_3^2)\ x/\varepsilon+(1-x/\varepsilon)^2\} \ ;$$

$$\zeta_e=(T_i/T_e)^{3/4}(m_e/m_i)^{1/4}\exp(U_i^2/2v_i^2) \quad ,$$

$$\zeta_i= 1 \quad ,$$

$$V = -\{ \sum_j s_j\zeta_j\alpha_j T_j(kU_i/\omega_r)/T_i+\beta_i\omega_r/kv_i\} \quad .$$

and κ_3 is read as $\tilde{\kappa}_1$ for meandering particles, $\tilde{\kappa}_2^{-1}$ for noncrossing particles, $\tilde{\kappa}_1$ and $\tilde{\kappa}_2$ satisfy the equations $w_D^m(\tilde{\kappa}_1)=\omega_r/k$, $w_D^n(\tilde{\kappa}_2)=\omega_r/k$, respectively, H(a) is the Heaviside's function

$$H(a) = \begin{cases} 1 \ , & a > 0 \\ 0 \ , & a < 0 \ . \end{cases}$$

Because the mode has its phase velocity between the drift velocities of ion and electron;

$$U_i < \omega_r/k < U_e \quad ,$$

the term relating to electrons is positive and that relationg to ions is negative. Then it can be seen that the drifting electrons give their kinetic energy to the wave and cause the instability in the magnetic neutral sheet while the ions absorb the energy from the wave.

6. Analytical and numerical estimates of growth rate

We can analytically solve the real and the imaginary parts of the dispersion relation in the extreme cases.

In the case of the small drift velocity, i.e. $|U_i|<<v_i$, eq.(39) is explicitly solved to give the following two branches:

$$\omega_r \simeq kU_i + k\{0.35[1+(T_e/T_i)^{-3/4}(m_e/m_i)^{1/4}]v_i$$

$$+\sqrt{2}(r^*_{Li}/\lambda)(1+T_e/T_i)^{-1/2}v^*_A\} \quad , \tag{42}$$

and

$$\omega_r \simeq kU_i - k(T_e m_e/T_i m_i)^{1/4}U_i \quad , \tag{43}$$

where v^*_A is the Alfvén velocity outside the sheet region. The mode (42) is propagating in the electron-drift direction while the other mode (43) is in the ion-drift direction. The phase velocity of the latter mode, however, hardly satisfies the condition $\omega_r/k << |U_i|$. Therefore we only consider the former mode as meaningful. The damping rate in this case mainly based on the ion contribution and is approximately given by

$$\gamma \simeq -0.2\ [1+(T_e/T_i)^{-3/4}(m_e/m_i)^{1/4}]|k|v_i \quad . \tag{44}$$

Both the real frequency and the damping rate depend on the temperature ratio weakly.

In the opposite extreme case, i.e. $|U_i| >> v_i$, the formula ${}_1F_1(\alpha,1;z) \simeq e^z z^{\alpha-1}/\Gamma(\alpha)$ can be used. Then we can solve the dispersion relation

$$\omega_r \simeq a_1 k v_i (r^*_{Li}/\lambda)\{1+2^{-1/4}(T_e/T_i)^{-3/4}(m_e/m_i)^{1/4}(\lambda/r^*_{Li})^{1/2}\} \quad . \tag{45}$$

Here a_1 is a numerical factor which is about 0.66. The real part again only weakly depends on the temperature ratio. On the other hand the growth rate in this case strongly depends on the temperature ratio. When $T_e/T_i > 1$, the source term due to drifting electrons are dominant and the growth rate is

approximately

$$\gamma \simeq \pi^2 |\omega_r| (T_e/T_i)^{-1/4} (m_e/m_i)^{3/4} (r^*_{Li}/\lambda)^{1/2} \left(1 - \frac{1}{2} \frac{T_i}{T_e} \frac{\lambda}{r^*_{Li}} \frac{\omega_r}{kv_i}\right)$$
$$\times \{a_2 (r^*_{Li}/\lambda)(kv_i/\omega_r) + a_3\}^{-1}, \qquad (46)$$

where numerical factors a_2, a_3 are about 6.3 and 3.9, respectively.

In the intermediate cases, where the drift velocity is comparable with the thermal velocity, the wave source due to electrons and the sink due to ions are both important, so that the whole system of eqs.(39) and (41) should be numerically analyzed.

The numerical results are shown by solid lines in Fig.6 for some temperature ratios T_e/T_i. In the same figure we show the analytical approximations for the extreme cases by broken lines. The analytical results depend more weakly on the thickness than the numerical ones, and this seems due to the neglect of the ion contribution in the analytical treatment. The critical value of λ is decreased as the temperature ratio is increased. Fig.7 shows how the temperature ratio T_e/T_i affects the growth rate. In this figure the numerical results are also shown by solid lines in comparison with the values of approximated expressions which are shown by broken lines. The growth rate has its maximum at $T_e/T_i \sim 2$-3. Note that the mode can grow even if $T_e = T_i$. When the sheet thickness becomes thin, γ becomes positive in a wide range of the ratio T_e/T_i.

Physically may be described this situation as follows. Based on the electromagnetic nature of the wave, the phase

velocity of the mode seen by the ions, $(\omega_r/k)-U_i$, becomes large as the thickness λ is reduced. Then the number of the coupled ions becomes small. Moreover because the mode is propagating in the direction of the electron-drift U_e, the coupled ions are separated into two families, meandering and noncrossing ions. As is described before, these noncrossing particles are hardly influenced by the perturbed electric field. By the effect of the reduced thickness a large amount of the coupled ions are in this family. Then absorber of the perturbed energy is greatly reduced when the sheet becomes thin enough. As to electrons, however, the thickness λ is still larger than r^*_{Le} so that the coupled-electron contribution is not so influenced. Consequently the instability occurs in a thin sheet. In the case of the large temperature ratio the contribution of the drifting electrons as the wave source is reduced. Because the phase velocity is slower than the electron thermal velocity, the gradient of the drift-Maxwellian distribution function seen by the wave becomes less steep when the temperature ratio becomes large. Then the drifting electrons cannot give much energy to the wave. On the other hand when the temperature ratio becomes small, the drift velocity U_e seen by the wave becomes small and the ion contribution becomes large. Then the growth rate is greatly reduced. As a result the wave has a suitable range of T_e/T_i for the positive growth rate.

7. Concluding remarks

It must be emphasized that the plasma contained in the neutral sheet region behaves in an entirely different way from the homogeneous or slightly inhomogeneous plasmas. One of the main features comes from the variety of the particle orbits; particles exhibit different orbits corresponding to different ε and p. Another point of difference is due to the structured configuration of the magnetic field which is not translationally invariant along the x-direction, so that the velocity space is always defined in connection with the real space. Starting from the neutral sheet region, only some part of energetic particles can feel outside of the sheet structure while the rest, with lower energies, of the particles will always remain in the neighbourhood of the null plane to make bouncing inside the sheet region. These low energy particles can easily be accelerated by the electric perturbation excited perpendicularly to the magnetic lines of force. The electromagnetic perturbation around the neutral sheet is found to form an eigenmode defined by the structrue, and is mainly contributed from the meandering particles.

Although the reconnection process is a macroscopic phenomenon, which is mainly caused by the piling up of the magnetic lines of force around the null plane, microinstability is essential to make the layer dissipative. When the half-thickness of the sheet is reduced down to 0.9 r^{*}_{Li} or less, the present mode becomes unstable. This implies that the instability considered here may play an important role to trigger the whole

macroscopic reconnection process of the thin neutral sheet, where the electron temperature and the ion temperature are comparable. If we take the typical field strength at the geomagnetic tail, B~20 gamma [3], and take λ/r^{*}_{Li}~2/3 as for the half-thickness of the sheet, the ion cycltron frequency ω^{*}_{ci}~2 rad/sec and eq.(45) gives ω_r~kv_i. When we assume $k\lambda$~0.2 and γ/ω_r~2×10^{-3}, the typical time scale of this instability is about 800 sec. (14 min.). This value coincides with the observed flare time scale [3].

Acknowledgement

The author would like to acknowledge the continuing guidance and encouragement of Professor H. Obayashi. He is grateful to Professor Y. Terashima and Professor H. Wilhelmsson, Chalmers University of Technology, Sweden, for their valuable discussions and criticism. Special thanks to Dr. M. Kako, Osaka University, for his helpfull advice and critical readings of the manuscript.

Figure Captions

Fig.1 Geometry of a plane neutral sheet. The current J_0 flows in the negative y direction. The yz- plane at x=0 is the magnetic null plane.

Fig.2 The ε-p phase space. All the particles exist in the region $\varepsilon \geq -p$. The particles which start at the position of x are limited in the rigion $\varepsilon \geq |p-A_j(x)|$. Meandering particles are in region I (shaded) and non-crossing particles in region II (hatched). Broken lines show the contours of the drift velocity w_D. The trajectory of no drift $w_D=0$ is shown by a dot-dash line.

Fig.3 Particle orbits in the vicinity of the null plane. A noncrossing orbit is shown in the left. The middle one is a meandering orbit drifting in the same direction as the noncrossing orbit. The right is another meandering orbit which drifts in the opposite direction.

Fig.4. The ε-p phase space, same as Figure 2. Broken lines show contours of normalized distribution function $\overline{F_i}$ $=\exp\{-(\varepsilon^2-2s_jU_jp)/2v_j^2\}$ for $|U_j|=v_j$. The region below the two-dot-dash line corresponds to $|x| \leq \lambda$.

Fig.5 Approximation of the equilibrium magnetic field used in the estimate of the orbit-integral. The equilibrium state is separated into two regions: the inner region, $|x| \leq \lambda$, where the strength of the field varies linearly and the outer region, $\lambda < |x|$, where the field is constant.

Fig.6 Growth rate normalized by ω_r versus the half-thickness of the sheet λ normalized by r^*_{Li}. Solid lines show the numerical results, and broken lines show the analytical approximations. Temperature ratio T_e/T_i is indicated by an attached figure to each curve. The growth rate becomes positive as the layer becomes thin enough.

Fig.7 Growth rate normalized by ω_r versus termperature ratio T_e/T_i. Solid lines show the numerical results and broken lines show the analytical approximations. Sheet thickness is indicated to each curve. The difference between numerical and analytical results comes from the neglect of ion contribution.

References

1. Sweet, P.A., in Electromagntic phenomena in cosmical physics (ed. B. Lehnert) P.123, Cambridge University Press, London, 1958.
2. Nishida, A. and Fujii, K., Planet. Space Sci. 24, 849 (1976).
3. Alidiered, M., Aymar, R., Jourdan, P., Koechlia, F. and Samain, A., Plasma Phys. 10, 841 (1968).
4. Ohyabu, N., Okamura, S. and Kawashima, N., Phys. Fluids 17, 2009 (1974); Baum, P.J. and Brateuahl, A., Phys. Fluids 17, 1232 (1974); Overskei, D. and Plitzer, P.A., Phys. Fluids 19, 683 (1976).
5. Kadomtsev, B.B., Fiz. Plazmy 1, 710 (1975).
6. Dungey, J.W., Cosmic Electrodynamics, p.48. Cambridge University press, London, 1958.
7. Parker, E.N., Astrophys. J., Suppl. Ser., 8, 177 (1963).
8. Petscheck, H.E., in AAS-NASA symposium on the physics of solar flare, p.425, 1964.
9. Friedman, M. and Hamberger, S.M., Solar Phys. 8, 104 (1969).
10. Yeh, T. and Axford, W.I., J. Plasma Phys., 4, 207 (1970).
11. Biskamp, D., Sagdeev, R.Z. and Schindler, K., Cosmic Electrodyn. 1, 297 (1970).
12. Galeev, A.A. and Zelenyi, L.M., Sov. Phys. JETP, 42, 450 (1975).
13. Schindler, K., J. Geophys. Res., 79. 2803 (1974).

14. Galeev, A.A. and Zelenyi, L.M., Sov. Phys. JETP, 43, 1113 (1976).

15. Harris, E.G., Nuovo Cimento 23, 115 (1962).

16. Seymour, P.W., Aust. J. Phys. 12, 309 (1959).

17. Hoh, F.C., Phys. Fluids 9, 277 (1966).

18. Magnus, W., Oberhettinger, F. and Soni, R.P., Formulas and Theorems for the Special Functions of Mathematical Physics, p.166, Springer-Verlag, Berlin, 1966.

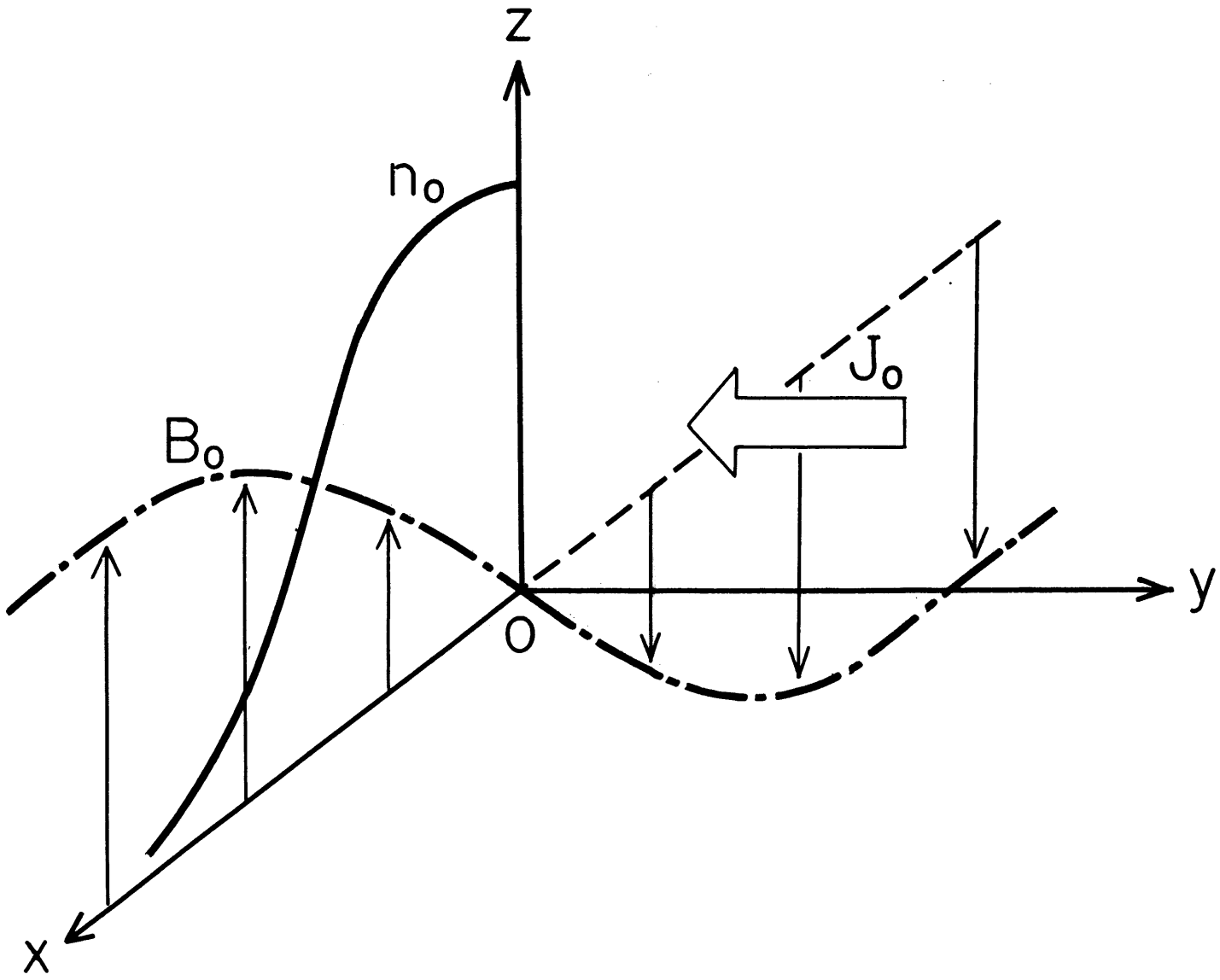

FIG. 1

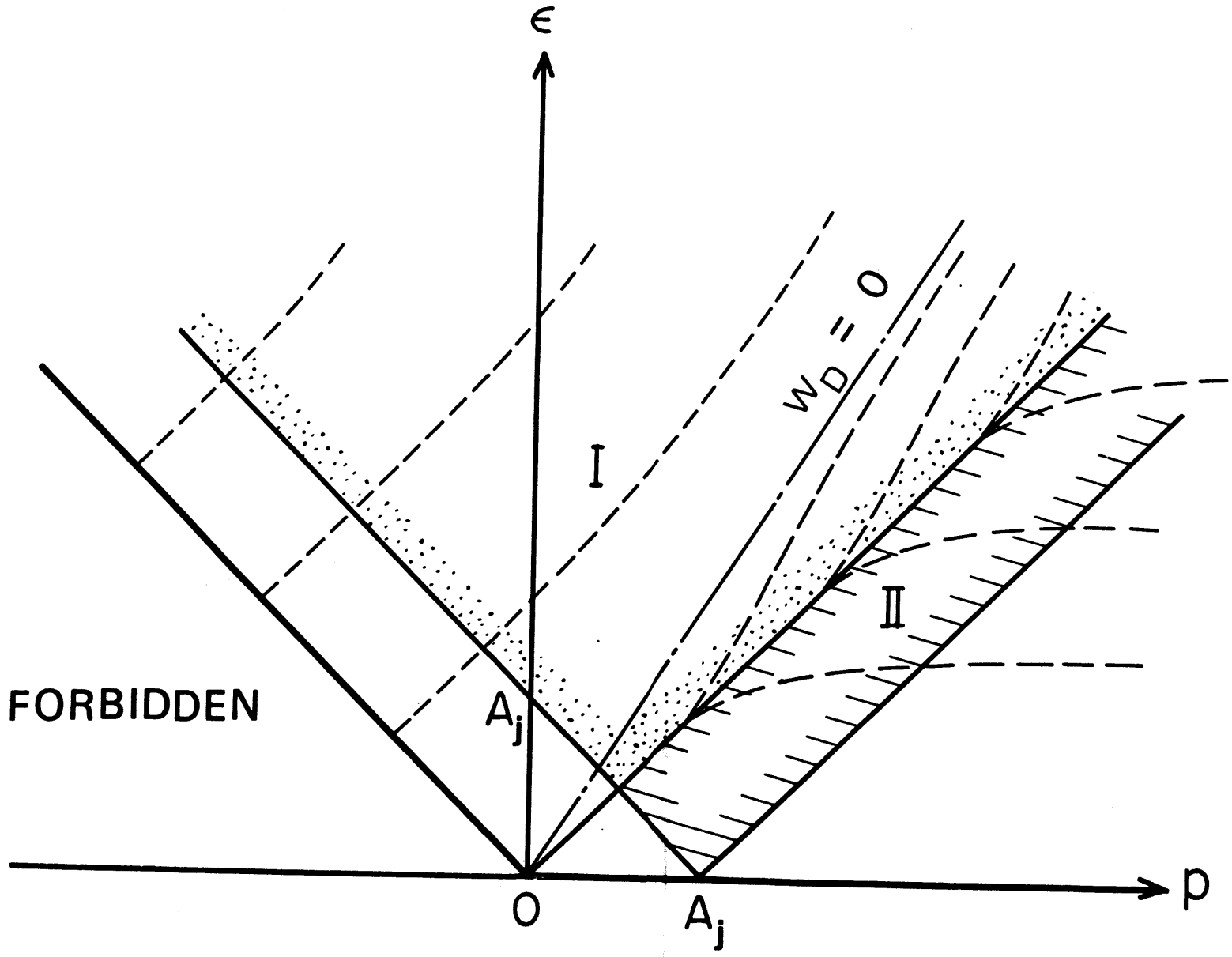

FIG. 2

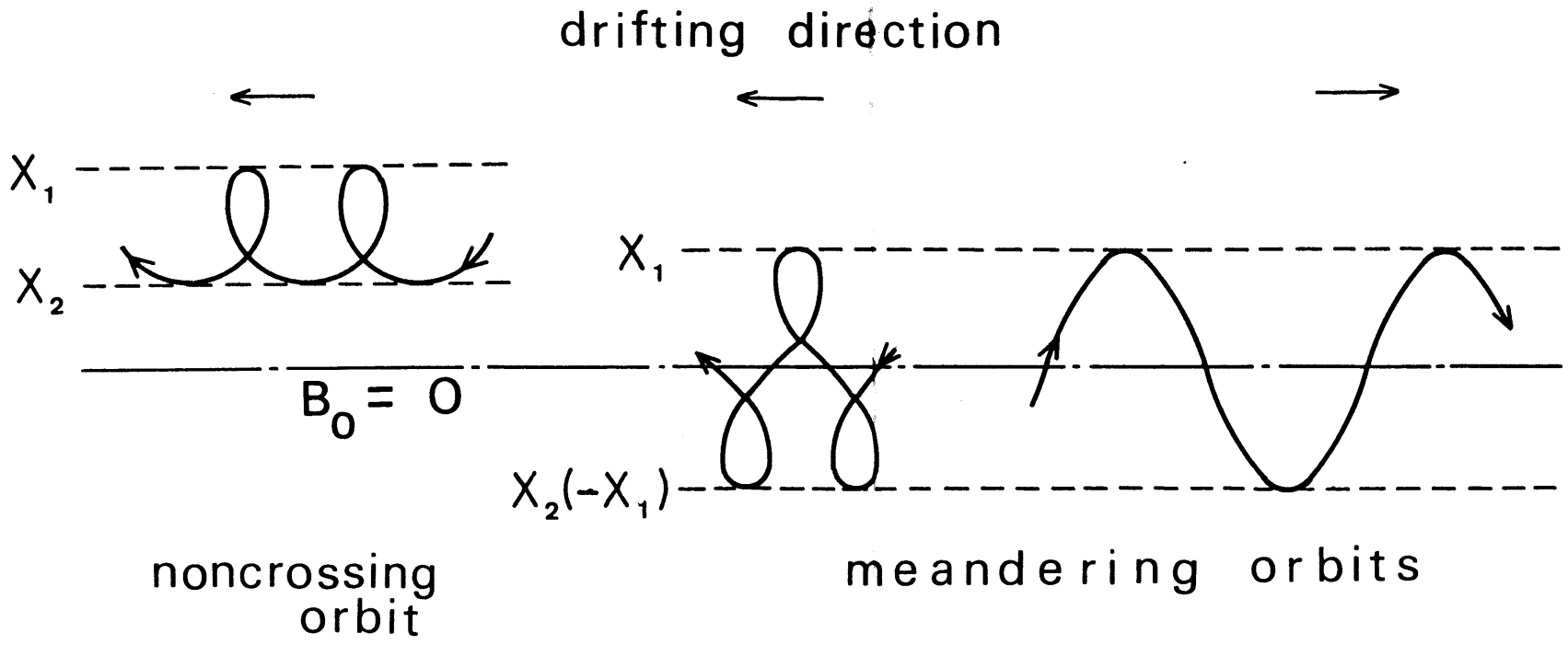
drifting direction
X1
X2
B0 = 0
X1
X2(-X1)
noncrossing orbit
meandering orbits

FIG. 3

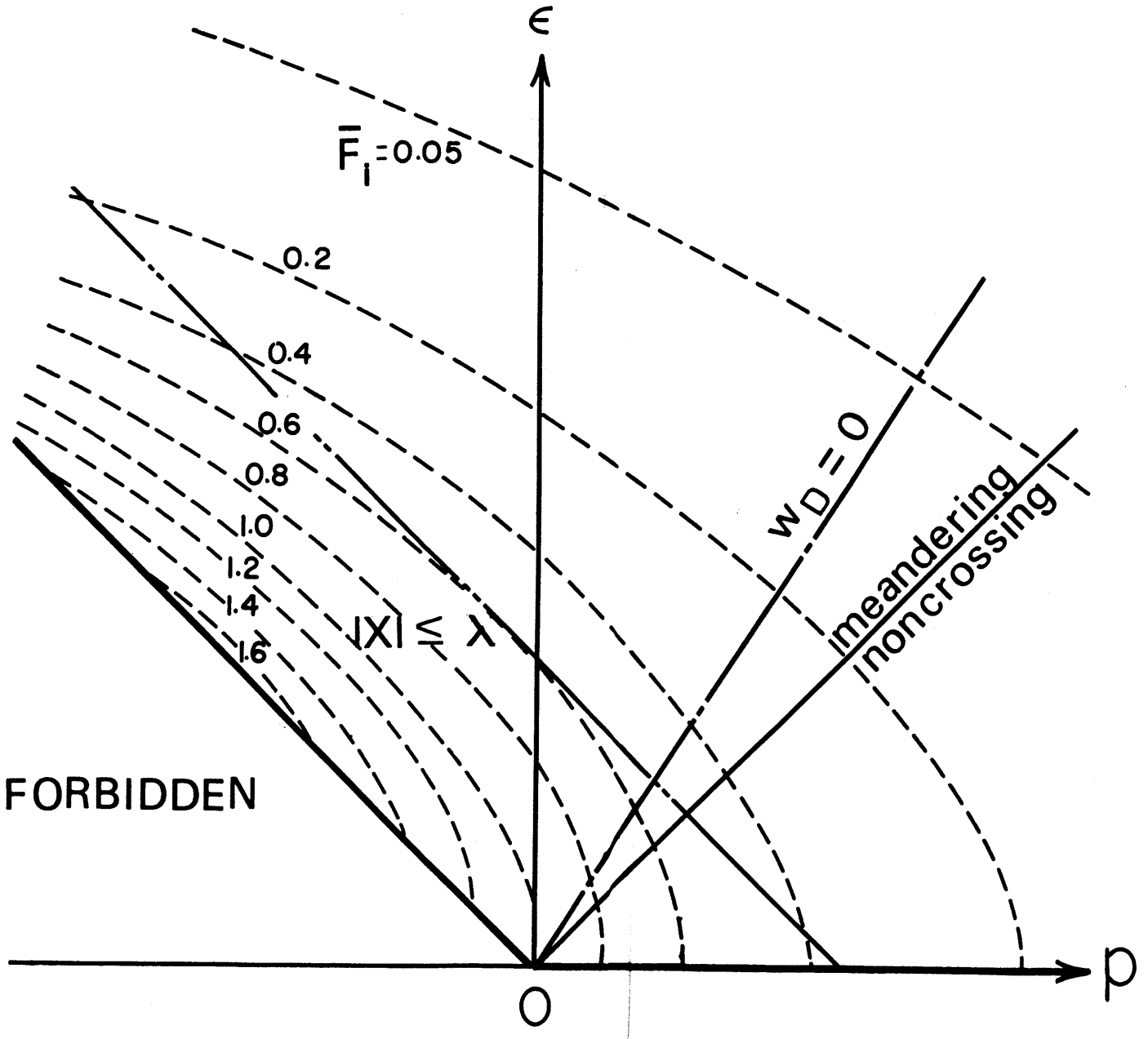
ϵ
$\bar{F}_1$=0.05
0.2
0.4
0.6
0.8
1.0
1.2
1.4
1.6
$w_D = 0$
meandering
noncrossing
$|X| \leq \lambda$
FORBIDDEN
0
p

FIG. 4

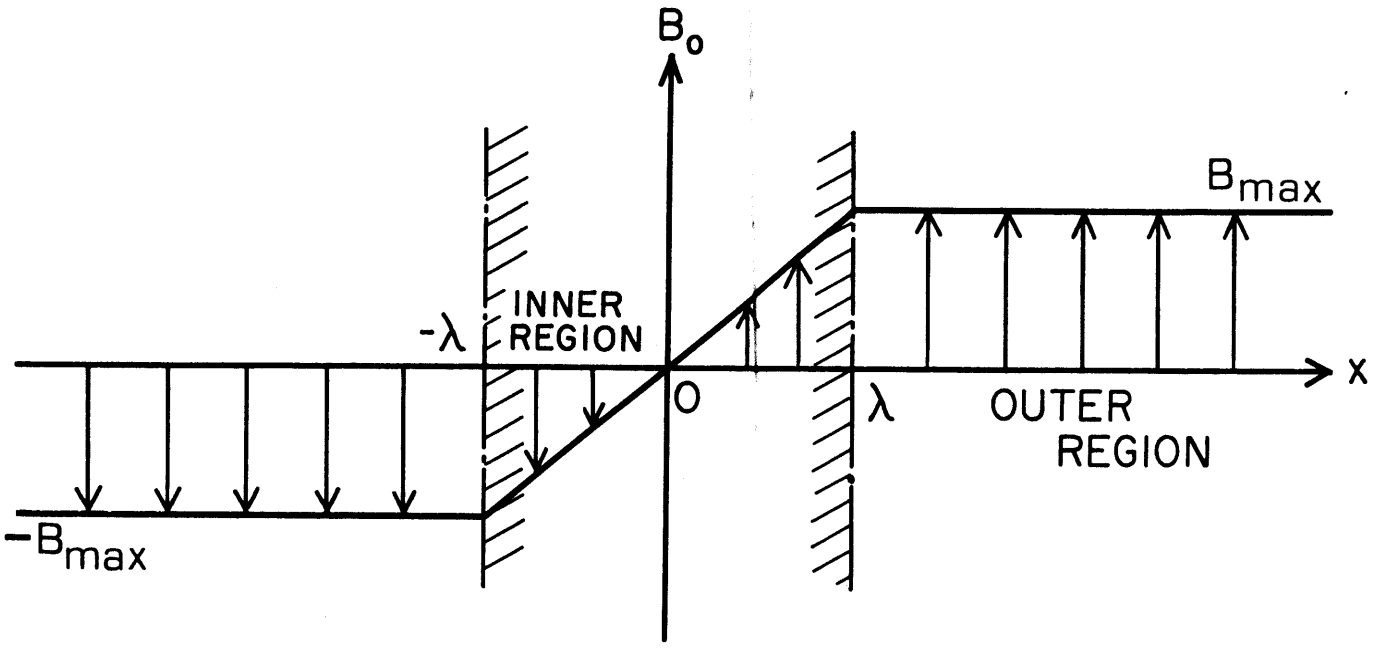

FIG. 5

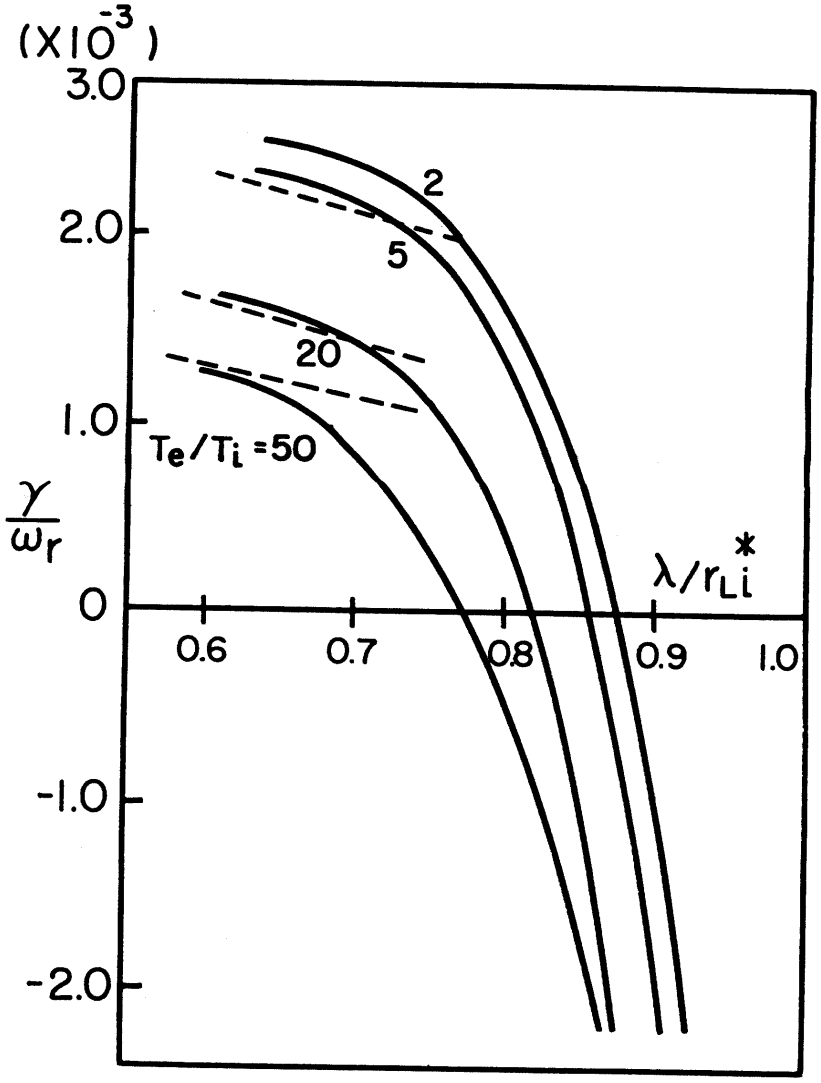

FIG. 6

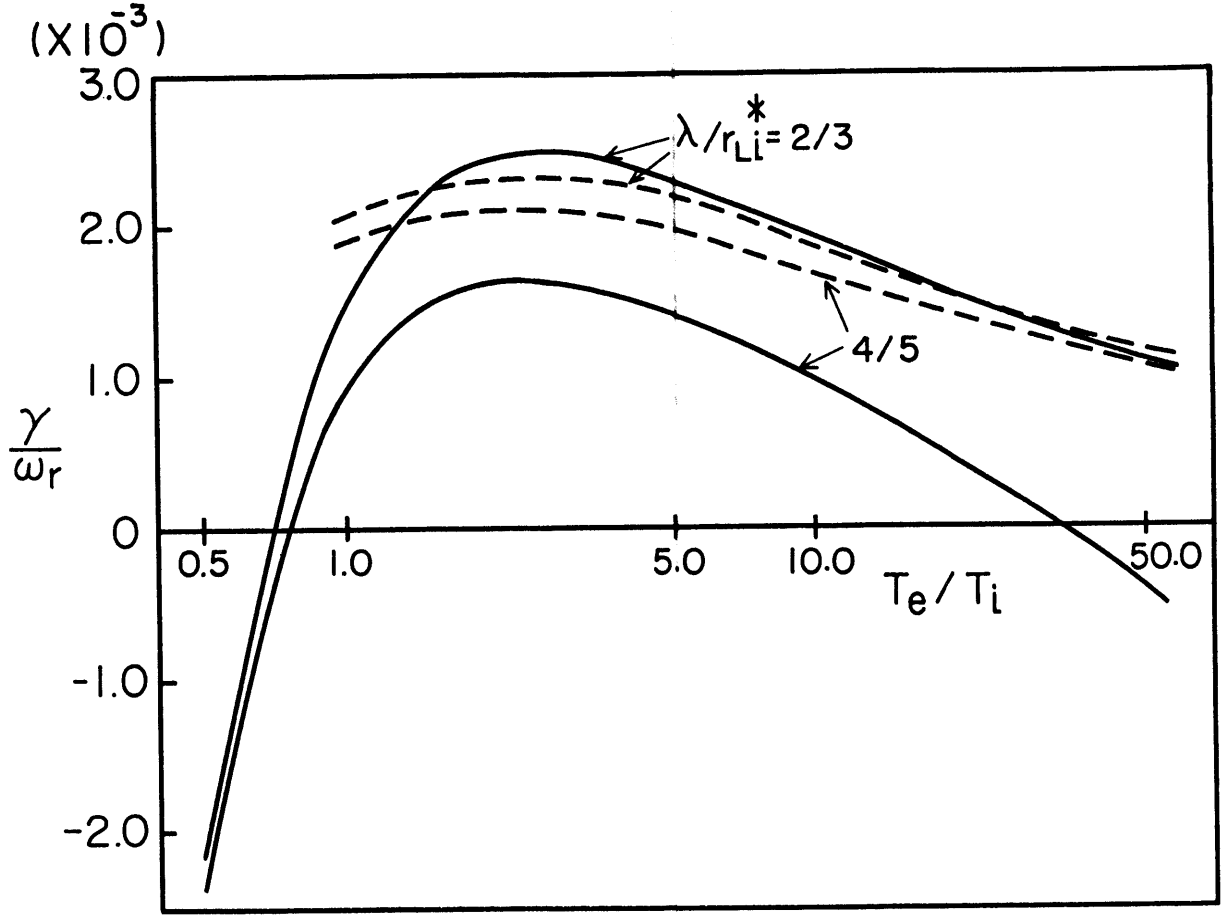

FIG. 7